CORE SIM+ SIMULATIONS OF COLIBRI FUEL RODS OSCILLATION EXPERIMENTS AND COMPARISON WITH MEASUREMENTS

A. G. Mylonakis[1,], **C. Demazière**[1], **P. Vinai**[1], **V. Lamirand**[2,3], **A. Rais**[2], **O. Pakari**[2]
P. Frajtag[2], **D. Godat**[2], **M. Hursin**[2,3], **G. Perret**[3], **A. Laureau**[2], **C. Fiorina**[2], **A. Pautz**[2,3]

[1]Chalmers University of Technology
Department of Physics
Division of Subatomic and Plasma Physics
SE-412 96 Gothenburg, Sweden

[2]École Polytechnique Fédérale de Lausanne
Laboratory for Reactor Physics and Systems behaviour
CH-1015 Lausanne, Switzerland

[3]Paul Scherrer Institute
Nuclear Energy and Safety Research Division
CH-5232 Villigen, Switzerland

{antmyl,demaz,vinai}@chalmers.se
{vincent.lamirand,adolfo.rais,oskari.pakari,pavel.frajtag,daniel.godat,mathieu.hursin}@epfl.ch
gregory.perret@psi.ch & {axel.laureau,carlo.fiorina,andreas.pautz}@epfl.ch

ABSTRACT

At EPFL, the CROCUS reactor has been used to carry out experiments with vibrating fuel rods. The paper presents a first attempt to employ the measured data to validate CORE SIM+, a neutron noise solver developed at Chalmers University of Technology. For this purpose, the original experimental data are processed in order to extract the necessary information. In particular, detector recordings are scrutinized and detrended, and used to estimate CPSDs of detector pairs. These values are then compared with the ones derived from the CORE SIM+ simulations of the experiments. The main trend of the experimental data along with the values for some detectors are successfully reproduced by CORE SIM+. Further work is necessary on both the experimental and computational sides in order to improve the validation process.

KEYWORDS: Neutron noise, research reactor, fuel rod vibration, code validation

1. INTRODUCTION

Neutron noise in power nuclear reactors consists of neutron flux fluctuations which are small in comparison with the main trend of the neutron flux. The perturbations, which act as neutron noise sources, can be problematic for the operation of nuclear reactors, and their effects need to be monitored and analyzed. The corresponding induced neutron noise can also be used to make a fingerprinting of the reactor core and early detect anomalies while the reactor is operating.

Recently, the need for identifying the causes of the increased neutron noise levels in some operating reactors, led the scientific community to make efforts to develop computational capabilities for neutron noise simulations. Neutron noise simulators computes the system response to a given perturbation. For their validation, it is therefore fundamental to have experimental data in which the neutron noise sources are well defined and known. One experimental program that aims at generating these types of data is the COLIBRI program in the CROCUS research reactor, at École Polytechnique Fédérale de Lausanne. In these experiments prescribed perturbations are imposed via a device that oscillates a group of up to eighteen fuel rods of the reactor core, mimicking fuel pin or assembly vibrations.

This work presents the analysis of the data generated with COLIBRI, along with a first attempt to validate CORE SIM+, a neutron noise solver developed at Chalmers University of Technology. The structure of the paper is as follows. Section 2 describes briefly the CROCUS reactor and the COLIBRI experimental set-up. Section 3 discusses the analysis of the experimental data. In Section 4, the numerical simulation of the experiments is described. Section 5 presents the comparison between the computational and the experimental results. In Section 6, conclusions are drawn.

2. THE CROCUS REACTOR AND THE COLIBRI FUEL RODS OSCILLATION EXPERIMENTS

The CROCUS reactor [1] is a uranium-fueled water-moderated reactor with an allowed maximum power of 100 W. It can thus be considered as a zero-power reactor. The core is approximately cylindrical in shape with a diameter of about 58 cm and a height of 100 cm. The active core region is partially submerged in water. The water level is allowed to vary for the control of the core reactivity. Two control rods containing boron carbide pellets are also used to control the reactor operation. The core is radially separated in two zones with different types of fuel. The central zone consists of 336 UO_2 fuel rods (with a 1.806 % enrichment) which are arranged in a square lattice with a pitch of 1.837 cm. The peripheral zone is loaded with 176 U metal fuel rods (0.947 % enriched) which are positioned in a lattice with a pitch of 2.917 cm. The first COLIBRI experimental campaign for CORTEX [2] includes a set of experiments where eighteen of the metallic uranium fuel rods are oscillated laterally (along the west-east direction), as illustrated in Figure 1a. A device composed of two moving plates is used to oscillate the fuel rods, as Figure 1b shows [3]. The two moving plates are respectively located above and below the upper and lower core grids, and are attached to the extremities of the eighteen fuel rods. The two plates are rigidly interconnected with an aluminum beam. The amplitude and the frequency of the oscillation are varied in the ranges of $\pm$ 0.5 - 2 mm and 0.1 - 2 Hz, respectively.

The reactor is equipped with eleven neutron detectors (Table 1) whose locations are displayed in Figure 1c. The detectors measure the neutron flux at their respective positions in time. Then the signals are recorded and stored by the data acquisition system (DAQ). From the analysis of the signals the neutron noise induced by the oscillating fuel rods is extracted.

3. ANALYSIS OF THE EXPERIMENTAL RESULTS

In this work, the COLIBRI experiments with identification numbers 12 and 13 [2] are selected to be analyzed. In both experiments the amplitude of the vibration is $\pm$ 2 mm. The frequencies of the
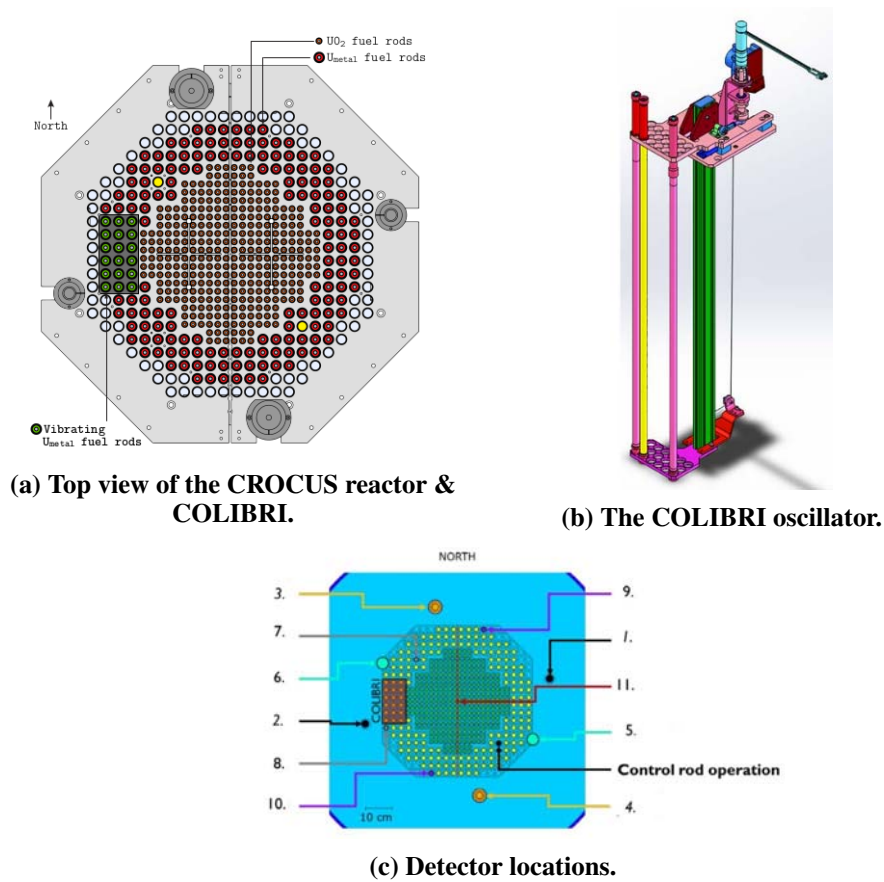
(a) Top view of the CROCUS reactor & COLIBRI.

(b) The COLIBRI oscillator.

(c) Detector locations.

Figure 1: The CROCUS reactor & the experimental setup.

Table 1: Detectors used in the COLIBRI experiments.

Detectors	Type	Operation mode	Additional use
1 and 2	^{235}U-coated compensated ionization chambers	pulse	safety monitors
3 and 4	^{10}B-coated compensated ionization chambers	current	operation monitors
5 and 6	^{235}U-coated fission chambers	current	-
7,8,9,10	^{10}BF$_3$ proportional counters	pulse	-
11	^{235}U-coated miniature fission chamber	pulse	-

vibrations are 0.1 Hz and 1 Hz, respectively. For the needs of the selected experiments, nine out of the eleven detectors are used, i.e. the ones with identification numbers 3 - 11 (Figure 1c).

The extraction of reliable information from the signals, requires the following steps: processing to prepare the signal in an appropriate form for further analysis, evaluation of the reliability of the used detectors and then the estimation of Cross-Power Spectral Density (CPSD) between the signals. These steps are described in the following subsections.

3.1. Processing of the detector signals

The neutron detectors provided time-dependent signals. The first processing step requires the removal of any possible trends from those signals since the measurements will be compared to frequency domain simulations assuming steady-state reactor operation. Afterwards, it is necessary to extract the neutron noise content. These two actions are performed by subtracting the rolling mean $\mu_{rolling}$ of the signal x, where the rolling mean is calculated using a sliding window over the detector signal. Finally, the signals from different detectors must be normalized. In this work, they are normalized to the static flux signal. A good representation of the static neutron flux is the rolling mean of the original signal. The whole processing phase reads as:

$$\delta x_{norm} = \frac{x - \mu_{rolling}}{\mu_{rolling}} \tag{1}$$

The signal of detector 3 from experiment 12 is used as an illustrating example of signal processing. That signal contains three linear trends, as Figure 2a shows. The impact of the signal trends is revealed in the corresponding histogram, where two overlapping normal distributions appear. The removed trend is depicted in Figure 2c. The processed neutron noise signal with no trend is then presented in Figure 2d. The new histogram (Figure 2e) confirms that the signal is now suitable for spectral analysis.
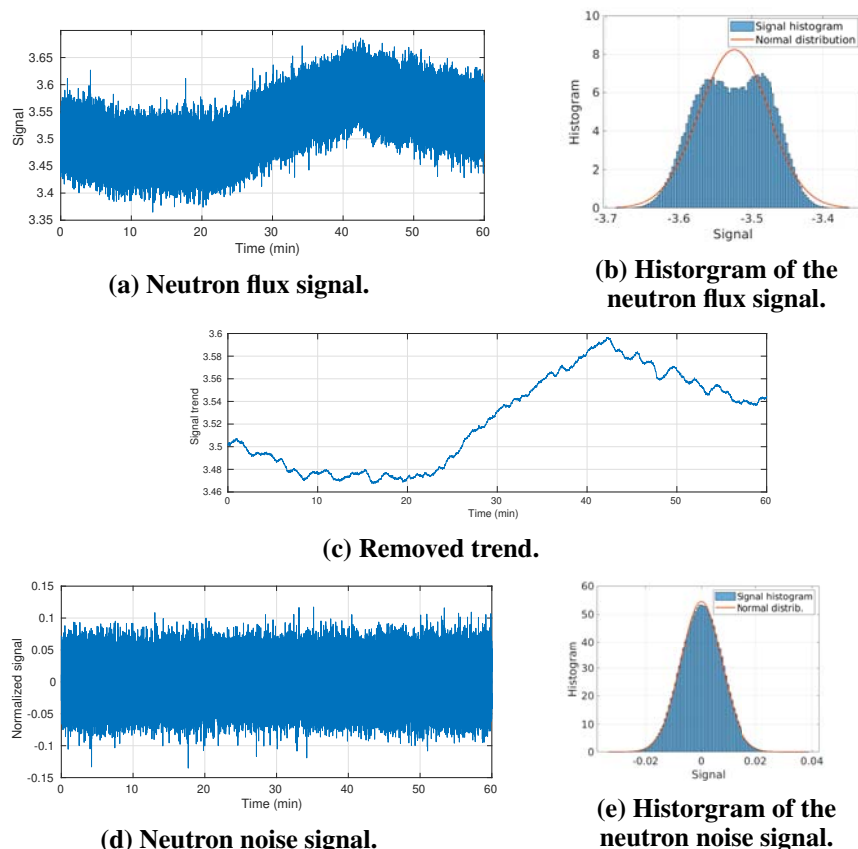

(a) Neutron flux signal.

(b) Historgram of the neutron flux signal.

(c) Removed trend.

(d) Neutron noise signal.

(e) Historgram of the neutron noise signal.

Figure 2: Detector 3 (experiment 12): Signal processing.

3.2. Evaluation of the detector reliability

Before proceeding to the extraction of the information from the available processed signals, the reliability of the detectors should be evaluated. For this purpose, the coherence between the signals is computed. The coherence provides a measure of how well the signal of one detector corresponds to the signal of another at each frequency. Figure 3 illustrates the coherence for some of the combinations of detector 3 with some other detectors in the case of experiment 12. It is clear that all combinations give a high coherence at the frequency of interest (0.1 Hz). On the other hand, the coherences of combinations with detector 11 are systematically low, as Figure 3 shows. This finding suggests that the detector 11 is not reliable. Thus, it is excluded from the analysis.
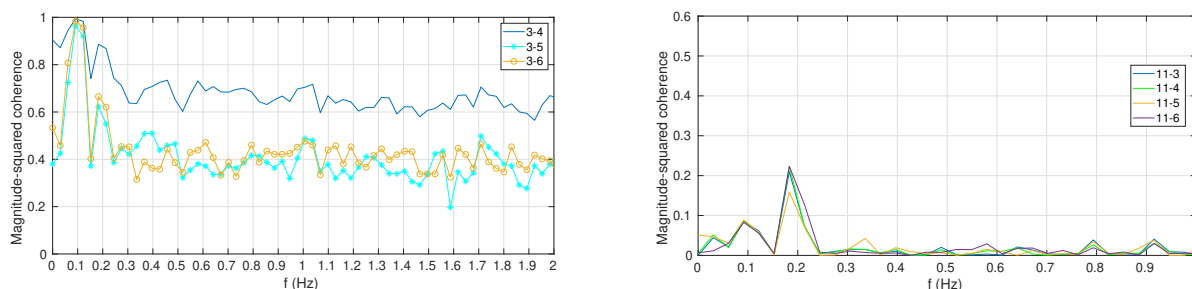

Figure 3: Coherence function for detectors 3 (left) and 11 (right).

3.3. Estimation of CPSDs between the detector signals

The detector signals 3 to 10 are considered reliable and are analyzed in the frequency domain. The Cross-Power Spectral Density (CPSD) is estimated with the Welch's method, for all combinations of detectors with detector 5. Table 2 reports the parameters used for the computation of the CPSDs. Then, the amplitude of CPSD between the detectors i and j at the frequency of interest f_0 is computed as the average CPSD amplitude under the peak at f_0. This is represented by the formula:

$$|CPSD_{i,j}|_{peak} = \frac{1}{f_a - f_b} \sum_{f_a}^{f_b} |CPSD(f)| \Delta f \tag{2}$$

where f_a and f_b are the boundaries of the frequency interval that includes the peak. All $CPSD_{i,j}$ amplitudes are normalized to the amplitude of $CPSD_{56}$. The phase of the CPSD is computed at the frequency of interest f_0. The experimental uncertainty associated with the amplitude and the phase of the peak is evaluated using the bootstrapping method.

Table 2: Parameters used for the computation of the experimental CPSD.

Window type	Window size	Overlapping	Dwell time (s)
Hann	8192	no	0.004

4. SIMULATION OF THE COLIBRI EXPERIMENTS

This section presents the simulation of the COLIBRI experiments with the CORE SIM+ neutron noise solver.

4.1. CORE SIM+

CORE SIM+ [4], is a neutron noise solver that is based on the two-energy-group kinetic neutron diffusion equations, capitalizing on the development of the former CORE SIM tool [5]. The calculation is arranged in two steps: first, the solver computes the steady-state neutron flux and second, it calculates the neutron noise in the frequency domain. The total space-dependent response of the reactor behavior is obtained by adding the neutron noise to the steady-state neutron flux. In CORE SIM+ a non-uniform mesh capability can be used to optimize the computational cost. In fact, fine mesh are necessary close to highly localized perturbations, where the gradient of the neutron flux can be strong. On the other hand, coarser meshes may be suitable for regions far from the perturbations. In addition, CORE SIM+ is equipped with various numerical methods for an efficient solution of both the criticality and the neutron noise problems [6],[7].

4.2. Modelling approach

A simplified 3-D model of the CROCUS reactor core [8] is used at this stage, as illustrated in Figure 4. The model consists of three homogenized regions: the inner fuel region, the outer fuel region and the water reflector. This modelling approach was demonstrated to be faithful enough, at least for reproducing the static neutron flux distribution [8]. The movement of the fuel rods imposed
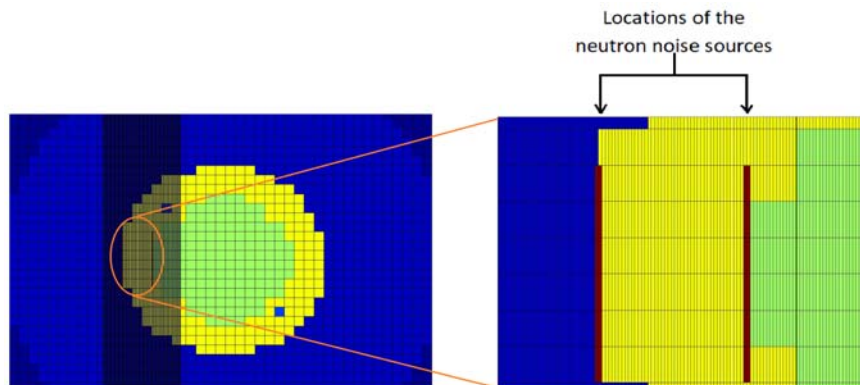

Figure 4: Radial cross-section of the reactor model (left) & neutron noise sources (right).

in the COLIBRI experiments is modelled with the ϵ/d method [9], [10]. Accordingly, the noise source is modeled as two Dirac-like perturbations introduced at the west and east boundaries of the region of the vibrating fuel rods (Figure 4). The amplitudes of the perturbations are defined as the differences in macroscopic cross-sections between the vibrating and the neighboring regions. A fine spatial discretization is used for the region where the perturbation is located, so that the effect of the small displacement of the fuel rods (corresponding to $\pm$ 2 mm in the current application) can be accurately reproduced.

The solver provides the spatial distribution of the neutron noise at each energy group, in the frequency domain. For the comparison with the experimental results, CPSDs are derived from the thermal neutron noise calculated at the locations of the detectors. The CPSD of the frequency domain neutron noise ($\delta\phi$) between the locations i and j is calculated with the following relation:

$$CPSD_{i,j} = \left(\frac{\delta\phi}{\phi_0}\right)_i \left(\frac{\delta\phi}{\phi_0}\right)_j^\dagger \qquad (3)$$

where $\dagger$ symbolizes the complex conjugate. To be consistent with the experimental results, all CPSD amplitudes are normalized to the amplitude of $CPSD_{56}$.

5. COMPARISON AND DISCUSSION

The experimental data of the COLIBRI tests 12 and 13 are compared with the respective simulations. In particular, the CPSDs between any detector and detector 5 are used. The amplitude and the phase values are plotted by distance from the oscillating fuel pins. The experimental results are reported with an uncertainty range that corresponds to $\pm 1\ \sigma$. The uncertainties associated with the phases are possibly underestimated. The reason is that the differences in signal treatment between detectors with different types of electronics is not taken into account.

As regards experiment 12, Figure 5a illustrates that the computed relative CPSD amplitudes of pairs 10-5, 9-5 and 5-5 are in agreement with the experimental ones. Concerning the pairs 8-5 and 4-5, the calculated amplitudes lie within a $\pm 2\ \sigma$ region from the experimental value. For the pairs 7-5 and 3-5, larger discrepancies are found. The CPSD phases are depicted in Figure 5b. The experimental and CORE SIM+ data show that all the detectors are rather in phase. The calculated phase of the pair 3-5 falls within the uncertainty interval of the experimental value. The phase predicted for the detector pairs 10-5, 3-5, 9-5 and 4-5 is very close to the experimental results, being the difference smaller than 3 degrees. For the detector pairs 6-5, 7-5 and 8-5, larger discrepancies are observed. The phase of $CPSD_{7,5}$ is higher than the one of $CPSD_{6,5}$ although the distance between the detectors 7 and 5 is shorter than the distance between the detectors 6 and 5. This indicates that a DAQ synchronization issue might be responsible for the observed deviations.

In experiment 13, Figure 5c illustrates that the experimental relative CPSD amplitudes of the pairs 7-5, 10-5, 9-5, 4-5 and 5-5 are satisfactorily estimated with CORE SIM+. The differences between experimental and simulated values for detectors 3 and 8 are found to be larger than the experimental uncertainty. The CPSD phases are given in Figure 5d. The experimental values show that all the detectors are rather in phase, a feature that is reproduced by the CORE SIM+ calculation. There is however a shift of 5-15 degrees of the calculated phases in comparison with the experimental ones. The measured phase for detector 8 is well predicted with the simulation, but the experimental uncertainty band associated to the detector is relatively large.

In both experiments, the amplitude curve has a local minimum at the CPSD pair 3-5. This might indicate a biased behavior of the detector 3. This observation agrees with the fact that the detectors 3 and 4 are the operation monitors of the reactor and their transfer functions have not been defined accurately.

The computational prediction of the $CPSD_{8,5}$ amplitude lies rather far from the experimental value, in both cases. A possible explanation is that the detector 8 is located very close to the noise source,

being sensitive to spectral effects, i.e. changes in the local neutron spectrum in addition to the overall flux oscillation. Moreover, the use of the neutron diffusion approximation in CORE SIM+ close to the noise source might be questionable.

Some aspects of the comparison between measurements and simulations will require additional analyses. On the computational side, a quite simple model with large homogenized regions is applied. Although the model is able to reproduce the main static features of CROCUS [8], its suitability for neutron noise calculations should be further investigated. Finally, the adequacy of the diffusion approximation for the simulation of localized noise sources, is still an open matter of research [11]. On the experimental side, a methodology is developed to reduce uncertainties [12]. The uncertainty reduction is also one of the priorities of the second COLIBRI campaign.
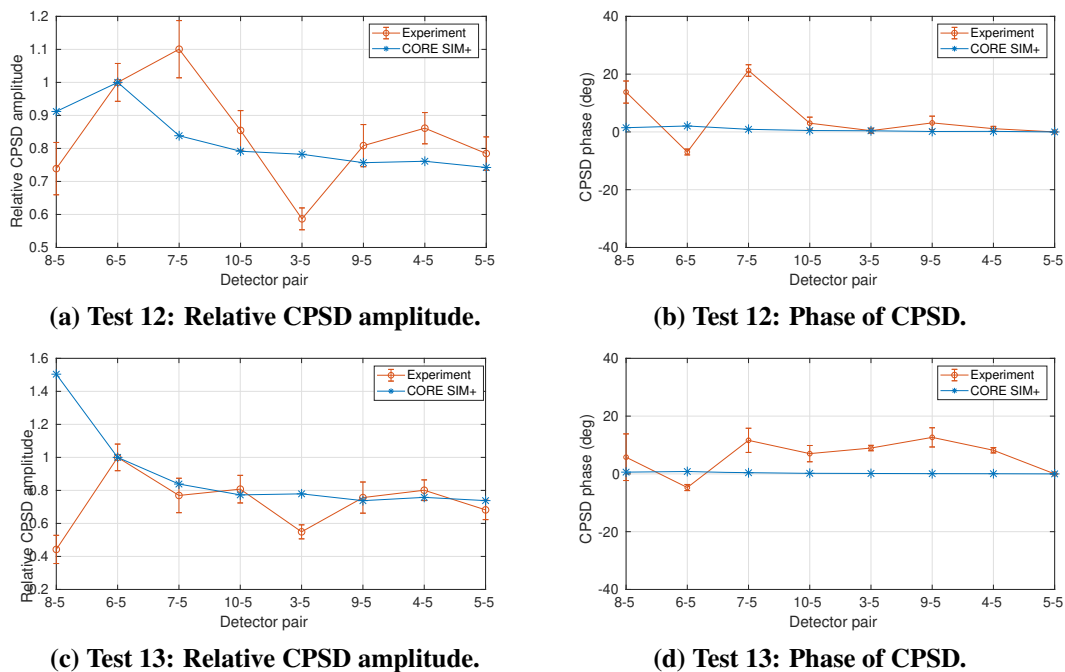

(a) Test 12: Relative CPSD amplitude.

(b) Test 12: Phase of CPSD.

(c) Test 13: Relative CPSD amplitude.

(d) Test 13: Phase of CPSD.

Figure 5: Comparison of the computational results with experimental data.

6. CONCLUSIONS

The paper presents the analysis of the data generated in the CROCUS reactor with the COLIBRI experiments, and their comparison with the simulations performed with CORE SIM+. The processing of the detector signals follows a sequence of steps in order to ensure that the signals have a proper form prior to their analysis. Significant trends were found to affect some signals, so they had to be removed. Then, the reliability of detectors is evaluated by examining their coherence functions. The trustworthy signals were analyzed in the frequency domain, experimental CPSDs between detectors pairs were derived and compared with the results of CORE SIM+. The comparison of the CPSD amplitudes shows that the majority of the reliable experimental values are reproduced satisfactorily by CORE SIM+. Most notably, the overall space dependence of the amplitude of the neutron noise with respect to the static flux is well reproduced by the simulations (with the exemption of the neutron noise in the close vicinity of the noise source, where the validity of diffusion theory is questionable). For the CPSD phases, the experimental and calculated data

show that the detectors are rather in phase with each other, despite the quantitative discrepancies. Such differences are however small in most cases. Additional studies are planned to evaluate the impact of experimental uncertainties and the approximations used in the modelling.

ACKNOWLEDGEMENTS

REFERENCES

[1] J. Paratte, R. Fruh, U. Kasemeyer, M. Kalugin, W. Timm, and R. Chawla. "A benchmark on the calculation of kinetic parameters based on reactivity effect experiments in the CROCUS reactor." *Annals of Nuclear Energy*, **volume 33**(8), pp. 739 – 748 (2006).

[2] V. Lamirand et al. "Experimental report of the 1st campaign at AKR-2 and CROCUS." Technical Report D3.1 (2018). URL http://cortex-h2020.eu/wp-content/uploads/2019/07/CORTEX_D2_1_Experimental_Report_of_the_1st_Campaign_at_AKR2_and_CROCUS_V1.pdf.

[3] V. Lamirand et al. "The COLIBRI programme in CROCUS: characterisation of the fuel rods oscillator." In *International conference on Advancements in Nuclear Instrumentation Measurement Methods and their Applications - ANIMMA*. Portoroz, Slovenia (2019).

[4] A. Mylonakis, P. Vinai, and C. Demazière. "Neutron noise modelling for nuclear reactor diagnostics." In *HNPS2018, the 27th Annual Symposium of the Hellenic Nuclear Physics Society*, pp. 139–143. Athens (2018).

[5] C. Demazière. "CORE SIM: A multi-purpose neutronic tool for research and education." *Annals of Nuclear Energy*, **volume 38**, pp. 2698–2718 (2011).

[6] A. G. Mylonakis, P. Vinai, and C. Demazière. "Numerical solution of two-energy-group neutron noise diffusion problems with fine spatial meshes." *Annals of Nuclear Energy* (2019). URL https://doi.org/10.1016/j.anucene.2019.107093.

[7] A. Mylonakis, P. Vinai, and C. Demazière. "Two-level multigrid preconditioning of a neutron noise diffusion solver." In *International Conference on Mathematics and Computational Methods applied to Nuclear Science and Engineering - M&C* (2019).

[8] A. Rais. *Performance assessement of a 3-D steady-state and spatial kinetics model for the CROCUS reactor*. Ph.D. thesis, École polytechnique fédérale de Lausanne (2017).

[9] C. Demazière and A. Dokhane. "Description of scenarios for the simulated data." Technical Report D3.1 (2019). URL http://cortex-h2020.eu/wp-content/uploads/2019/07/CORTEX_D3_1_Description_of_scenarios_for_the_simulated_data_V1.pdf.

[10] I. Pazsit and J. Karlsson. "On the perturbative calculation of the vibration noise by strong absorbers." *Annals of Nuclear Energy*, **volume 24**(6), pp. 449 – 466 (1997).

[11] A. Mylonakis, H. Yi, P. Vinai, and C. Demazière. "Neutron noise simulations: a comparison between a diffusion-based and a discrete ordinates solver." In *International Conference on Mathematics and Computational Methods applied to Nuclear Science and Engineering - M&C* (2019).

[12] V. Lamirand et al. "Analysis of the COLIBRI neutron noise campaign in the CROCUS reactor for the European project CORTEX." In *International Conference on Physics of Reactors - PHYSOR* (2020).